The Evolutionary Ecology of Individual Foraging Decisions

Pratik R. Gupte[1,*]

Christoph F. G. Netz[1]

Franz J. Weissing[1]

1. University of Groningen, Groningen 9747AG, The Netherlands.

∗ Corresponding authors; e-mail: p.r.gupte@rug.nl

Manuscript elements: EXAMPLE: Figure 1, figure 2, table 1, online appendices A and B (including figure A1 and figure A2). Figure 2 is to print in color.

Keywords: Examples, model, template, guidelines.

Manuscript type: Article.

Prepared using the suggested LaTeX template for *Am. Nat.*

Abstract

WORK IN PROGRESS

Introduction

WORK IN PROGRESS

Evolutionary Simulation Model of Individual Foraging Decisions

Our model is an individual-based evolutionary simulation whose most basic components — the environment size and shape, its gridded structure and each cell's capacity to hold multiple individuals, as well as the discrete conception of time within and between generations — is taken from Netz et al. *in prep.*. We conceptualised the model and the scenarios around the behaviour of waders (*Charadrii*, and especially oystercatchers *Haematopus sp.*), which are extensively studied in an optimal foraging context (e.g. Ens et al., 1990; Vahl et al., 2005*a*,*b*,*c*). We simulated a fixed population with a fixed size of 10,000 individuals moving on a landscape of 512^2 grid cells, with the landscape wrapped at the boundaries so that individuals passing beyond the bounds at one end re-appear on the diametrically opposite side. Individuals have a lifetime of T timesteps, with T set to 400 by default. After their lifetime, individuals reproduce and transmit their heritable traits proportional to their fitness over their lifetime. The model code (in C++) can be found as part of the Supplementary Material in the Zenodo repository at **Zenodo/other repository here**.

Flexibility in Foraging Strategies

Our model considers three main scenarios of flexibility in individual foraging strategies. The **first scenario** is an inflexible producer-only case, in which individuals move about on the landscape and probabilistically find and consume discrete prey food items. Between finding and consuming a food item, individuals must 'handle' the prey for a fixed handling time T_H which is constant across prey items. Prey handling time T_H is set at 5 timesteps by default. The handling time dynamic is well known from many systems; for instance, it could be the time required for a wader to break through a mussel shell, with the handling action obvious to nearby individuals,

and the prey not fully under the control of the finder. We refer to such individuals as 'handlers' for convenience. Handlers are assumed to be fully absorbed in their processing of prey, and do not make any movements until they have fully handled and consumed their prey. The **second scenario** is a fixed-strategy case which adds some flexibility. Individuals at the start of their lifetime each choose between two foraging strategies, which are then fixed through life. The strategy choice is based on local environmental cues, and is covered in "Movement and Foraging Decisions". The two strategies are to produce, i.e., to probabilistically find, handle, and consume discrete prey (as in the producer-only case), or to scrounge as a kleptoparasite, i.e., to steal a found prey item from the individual handling it. We refer to such scroungers as 'kleptoparasites' from here onwards. Kleptoparasites can steal from any handler, regardless of whether that handler acquired its prey by searching or theft. Kleptoparasites are always successful in stealing from the handler they target; this may be thought of as the benefit of the element of surprise, a common observation in nature. Having acquired prey, a kleptoparasite need only handle it for $T_H - t_h$ timesteps, where t_h is the time that the prey has already been handled by its previous handler. The targeted handler deprived of its prey is assumed to flee from the area, and does not make a further movement decision. Thus kleptoparasites clearly save time on handling compared to a producer, and the time saved increases with the handling time T_H of the prey. The **third scenario** is a flexible-strategy case, and individuals are allowed to be plastic in their foraging strategies, and choose between producing and scrounging strategies in each timestep. Apart from the frequency of the choice, the actual foraging dynamics are the same as described in the fixed-strategy case. Individuals move about on the environment, and each foraging strategy choice is based on local environmental cues (see "Movement and Foraging Decisions").

Movement and Foraging Decisions

Individuals essentially use cues available in timestep t to predict their best move for the next timestep $t+1$, and the strategy associated with that move (when this is allowed). The movement decision is based on three local environmental cues: (1) the number of discrete prey items G,

(2) the number of individuals handling prey H (referred to as 'handlers'), and (3) the number of individuals not handling prey P (referred to as 'non-handlers'). The notation is chosen in keeping with Netz et al. *in prep.*. These cues are available to individuals in all three model scenarios. Individuals occupy a single grid cell on the environment at a time, and assign a suitability score S incorporating G, H, and P per cell to the nine cells in their Moore neighbourhood (including their current cell). Following Netz et al. *in prep.*, individuals calculate the cell-specific S as

$$S = m_g G + m_h H + m_p P + m_b$$

where the weighing factors for each cue m_g, m_h and m_p, and the bias m_b are genetically encoded and heritable between generations. Individuals rank their Moore neighbourhood by S in timestep t and move to the highest ranked cell in timestep $t + 1$.

Individuals in the producers-only case make no foraging decisions and find food items probabilistically (see "Prey Environment and Ecological Dynamics"). In the fixed-strategy case, individuals pick a lifelong foraging strategy in their first timestep (t_0), while in the flexible-strategy case, individuals pick a strategy in each timestep t to be deployed in $t + 1$. Individuals in these latter two cases process the cell-specific environmental cues G, H, and P to determine their foraging strategy F for life (fixed strategy), or in the grid cell into which they have chosen to move in $t + 1$ (flexible strategy). F is determined as

$$F = \begin{cases} producer, & \text{if } f_g G + f_h H + f_p P + f_b \geq 0 \\ scrounger, & \text{otherwise} \end{cases}$$

where the cue weights f_g, f_h and f_p, and the bias f_b are also genetically encoded and heritable between generations.

In both latter cases that allow for kleptoparasitism, individuals make their foraging strategy choice for the next timestep after they have passed through the ecological dynamics of their current location. This excludes individuals that have been stolen from are an important exception; these fleeing agents are moved to a random cell within a Chebyshev distance of 5, and do not make a foraging decision there. Thus kleptoparasitism not only gains individuals prey items

while depriving the targeted individual, it also displaces a potential competitor. All individuals move simultaneously, and attempt to implement the foraging strategy chosen for their new location (see below).

Prey Environment and Ecological Dynamics

Since our model was initially conceived to represent foraging waders, we developed a resource landscape based on mussels (family *Mytilidae*) that are commonly found in inter-tidal systems. Mussels beds share some important characteristics with other discrete prey items. Firstly, mussels are immobile relative to their consumers, and their abundances are largely driven by extrinsic environmental gradients and very small-scale interactions (de Jager et al., 2020, 2011). Secondly, in common with many ecological systems (Levin, 1992), mussels are not uniformly distributed across the inter-tidal mudflats, and are instead strongly spatially patterned into clusters ('beds') (de Jager et al., 2020, 2011). Thirdly, while prey or their signs in an area are often visible to consumers, consumers are not always certain of obtaining one of these prey, since prey can show small-scale anti-predator avoidance responses.

We captured these essential aspects of prey dynamics when implementing the resource landscape on which our individuals move. We modelled relative prey immobility and extrinsically driven abundance by assigning each grid cell of the resource landscape a constant probability of generating a new prey item per timestep, which we refer to as the growth rate r. We modelled clustering in the abundance of prey by having the distribution of r across the grid cells take the form of 1,024 uniformly distributed resource peaks with r declining from the centre of each peak to its periphery (Figure X). Effectively, the cell at the centre of each patch generates a prey item five times more frequently than the cells at the edges. Thus for a simulation-specific baseline r_{base} = 0.03, the central cell of a resource peak would have an $r_{centre} = 0.03$, and generate 3 items every 100 timesteps, compared with $r_{edge} = 0.006$, or 0.6 items generated in 100 timesteps. We ran the simulation with r_{base} values of 0.001, 0.01, 0.03, and 0.05, which we considered a sufficiently broad range. Cells in our landscape were modelled as being able to hold a maximum of K prey

items, with the default $K = 5$. While a cell is at carrying capacity its r is 0. We modelled near-perfect intermediate-range perception but uncertain short-range acquisition of prey by allowing individuals to perceive all prey items G in a cell, but giving individuals which choose a producer strategy only a probability of finding one of these prey. The probability of finding a prey item $p(success)$ is given as the probability of not finding any of G prey

$$p(success) = 1 - (1 - p_i)^G$$

where p_i is the detection probability of each of G items, which is uniformly set to 0.2 by default for all items.

Since we model foraging events as occurring simultaneously, it is possible for more producers to be considered successful in finding prey than there are discrete items in that cell. We resolve this simple case of exploitation competition by assigning G prey among some N successful finders at random. Producers that are assigned a prey item in timestep t begin handling it, and are considered to be handlers for the purposes of timestep $t + 1$ (primarily movement and foraging decisions of other individuals). It is important to note that a producer that has converted into a handler in timestep t is not an available target for kleptoparasites until timestep $t + 1$. Producers that are not assigned a prey item are considered idle during timestep t, and are counted as non-handlers for $t + 1$.

Kleptoparasites in the fixed- or flexible-strategy case face a slightly different challenge. All kleptoparasites in a cell successfully steal from a handler, contingent on the number of handlers matching or exceeding the number of kleptoparasites in timestep t. When the number of kleptoparasites exceeds handlers, handlers are assigned among kleptoparasites at random. Successful kleptoparasites convert into handlers, and similar to producer-handlers are unavailable as targets to other kleptoparasites until the next timestep. Unsuccessful kleptoparasites are considered idle, and are also counted as non-handlers for timestep $t + 1$. A handler that finishes processing its prey in timestep t returns to the non-handler state and is assessed as such by other agents when determining movements for $t + 1$.

Individuals move and forage on the resource landscape for T timesteps per generation, and T is set at 400 by default. Handling a food item requires a maximum of T_H timesteps, during which the handler is immobile.

Reproduction and the Evolution of Decision Making

At the end of each generation, the population is replaced by its offspring, maintaining the fixed population size, and the decision-making weights which determine individual movement (m_g, m_h, m_p, m_b) and foraging strategy choice (f_g, f_h, f_p, f_b) are transmitted from parent individuals to offspring. The number of offspring of each parent is proportional to the parent's share of the population fitness, and this is implemented as a weighted lottery that selects a parent for each offspring. The total lifetime intake of individuals is used as a proxy of fitness, and the population's total fitness is its total intake. The decision-making weights are subject to independent random mutations with a probability of 0.001. The size of the mutation (either positive or negative) is drawn from a Cauchy distribution with a scale of 0.01 centred on the current value of the weight to be mutated. This allows for a small number of very large mutations while the majority of mutations are small. We recognised that spatial autocorrelation in the landscape coupled with limited natal dispersal can lead to spatial heterogeneity in evolved movement rules, as lineages adapt to local conditions. Furthermore, limited natal dispersal could lead to population-level movements due to differential reproduction that mirror shifts in resource abundance, rather than individual movement. To ensure that global individual movement rules evolved, we intialised each offspring at a random location on the landscape, and also reset its total intake to zero.

Simulation Output and Analysis

Spatial Distribution of Individuals, their Intake, and Prey Items. Over each of the last eight generations of the simulation (991 – 998), we summed the following for each grid cell ij over the generation's timesteps: (1) the number of prey items G, (2) the number of individuals following

each of the two strategies, producer N_p or kleptoparasitic scrounger N_s, and (3) the intake (in food items consumed after handling) by agents following each of the two strategies, producer I_p or kleptoparasite I_s. For instance, the number of producer individuals in a generation to inhabit a cell ij would be

$$N_p = \sum_{t=0}^{i=T} n_{p_t}$$

where $t \in (0, 1 \ldots T = 400)$, and n_{p_t} is the number of producers in cell ij at each timestep t. We saved this generation- and simulation- specific data to file, and these data are available at the Zenodo/IRODS repository at **Zenodo/other link here**. The volume of data at this stage was comparable to a very high-resolution, long-term ecological study, and we handled it accordingly. First, we processed the data to get the timestep-averaged values of G, N_p, N_s, I_p, and I_s for each cell, dividing each value by T (400). From this data, we calculated the per-capita intake rate (I per t) on each cell for each of the two strategies separately, which we denote as R_p (producers) and R_s (scroungers). We plotted the timestep- and generation-averaged item count (G), strategy count (N_p, N_s), and absolute and per-capita intake (I_p, I_s, and R_p, R_s) in relation to grid-cell quality (the growth rate, r) to investigate the spatial distribution of individuals (see Figure X).

Generalised Functional Response. In our simulation, individuals perceive and respond to the standing stock of prey items G on a cell rather than its growth rate r. This standing stock is unpredictable due to consumption by other individuals. To understand the consequences of movement, we needed to investigate how individual intake varies with G as well as the presence of potential competitors. Thus we examined the generalised functional response (W) *sensu*Meer and Ens (1997). We plotted the per-capita intake rate achieved by individuals on grid-cells with similar numbers of prey items (G) and individuals ($N_p + N_s$). We did this separately for W_p and W_s, i.e., the generalised functional response for producers and kleptoparasitic scroungers, respectively. We modelled the effect of competition and resource availability on W_p and W_s using a simple generalised linear model (GLM) with either W_p or W_s as the response, and the number of individuals and the number of prey items as the only additive predictors. We repeated this for

simulations with different baseline growth rates r, and examined variation in the contribution of competition and resource availability in the form of the linear model coefficients of individual density and item density, respectively. These linear models took the form

$$W = \beta_0 + \beta_1 G + \beta_2 (N_p + N_s)$$

where W is either W_p or W_s. We fit these models for each r_{base} separately, but did not distinguish between replicates.

Decision Making Weights. To understand the evolutionary consequences of our simulation, we exported the the decision-making weights which determine individual movement (m_g, m_h, m_p, m_b) and foraging strategy choice (f_g, f_h, f_p, f_b) of each individual in every generation of the simulation. We examined how the frequency of these weights changed over the simulation, i.e., how the weights evolved. We visualised weights' evolution after scaling them between -1 and +1 using a hyperbolic tangent function, and binning the scaled values into intervals of 0.1. We refer to these scaled and binned values as phenotypes for convenience. Weights at or near -1 would represent the maximum evolved avoidance of an environmental cue (in relation to a movement weight) or the greatest evolved negative effect of a cue on choosing the foraging strategy (in relation to a strategy choice weight). Similarly, weights at or near +1 represent the greatest evovled preference for or positive effect of a cue on the movement and strategy choice mechanism of an individual.

Simulation Model Outcomes

Emergence of a Dynamic Equilibrium

Evolution of Movement Decisions

Response to Prey Items. Populations across scenarios consistently evolved to move towards food items, with all individuals evolving positive values of m_g across regrowth rates (Fig. 1.a). How-

ever, across scenarios, replicates and growth rates, populations did not converge upon a single value of m_g, with a similar number of phenotypes evolved across replicates (Fig. 1.e). Scenarios 2 and 3 showed opposite relationships between the number of m_g phenotypes and r_{base}: in scenario 2, there were only about half as many phenotypes as in scenario 3 for $r_{base} \leq 0.1$, while at the highest r_{base} (0.25), there were almost four times as many phenotypes in scenario 2 as in scenario 3.

Response to Handling Individuals. Populations across scenarios evolved to move towards handling individuals at low growth rates, with most individuals in the final generation having positive values of m_h ($r_{base} < 0.05$; Fig. 1.b). At higher growth rates, populations in scenario 3 consistently evolved a preference for handling individuals, with variation in the number of phenotypes declining with increasing r_{base}(Fig. 1.b, f). In scenarios 1 and 2 however, the proportion of the population with an evolved preference for moving towards handling individuals declined at higher growth rates, with only between 25% and 50% of the population showing such a preference at the highest growth rate. This decreasing preference for handlers was accompanied by an increase in the number of negative phenotypes of m_h, though the number of positive phenotypes was maintained despite the lower proportion of individuals with a positive m_h.

Response to Non-Handling Individuals. Acros scenarios, populations evolved to move away from non-handling individuals when growth rates were low, with most individuals in the final generation having negative values of m_p ($r_{base} < 0.1$; Fig. 1.c). At higher growth rates, however, populations in scenarios 1 and 2 evolved no particular preference or avoidance of non-handlers, while in scenario 3 the population consistently evolved to move towards non-handling individuals. There was wide variation in the strength of avoidance (and at higher r_{base}, preference), with multiple m_p phenotypes (Fig. 1.g).

Overall Response to Individuals. On summing, transforming, and binning the weights for handling and non-handling individuals, the evolved preferences for individuals in total were distinct

to each scenario. Populations in scenario 3 evolved a consistent preference for moving towards individuals overall (Fig. 1.d).In scenario 2, the proportion of the population with an overall preference for moving towards individuals declined linearly with growth rate. At the two highest growth rates (0.1, 0.25), about 50% of fixed-strategy individuals preferred to move towards other individuals. Scenario 1 showed a strongly non-linear, inverse hump-shaped relationship between the preference for individuals and growth rates. At very low growth rates ($r_{base} \approx 0.001$), about half the population had an overall preference for moving towards other individuals. This proportion declined until nearly all individuals avoided each other when choosing where to move for $0.01 \geq r_{base} < 0.1$. Across high growth rates (≥ 0.1), an increasing proportion of individuals preferred to move towards other individuals overall (Fig. 2.d).

Evolution of Foraging Strategy

Populations in scenario 1 were fixed to choose a producer strategy, and their foraging strategy weights evolved neutrally, providing a null model of weight evolution against which to compare scenarios 2 and 3. Populations in scenario 3 did not show a consistently evolved bias towards choosing a producing strategy, with no discernible pattern in the proportion of the population bearing a positive f_b (Fig. 2. a). However, populations in scenario 2 showed an increasing proportion of individuals biased towards a foraging strategy with increasing r_{base}. At the highest growth rate, all evolved individuals in scenario 3 were biased towards producing (Fig. 2.a).

Populations across scenarios, growth rates, and replicates evolved to seemingly ignore prey items and non-handling individuals when making a foraging decision, with no consistency in the proportion of individuals bearing positive f_g and f_p across replicates of the same scenario and growth rate(Fig. 2.b,d). Howevever, evolved populations in scenario 3 were more likely to uniformly choose a foraging strategy based on the number of non-handling individuals, with more variation within rather than between growth rates.

The number of handling individuals was not processed similarly by individuals evolved in scenario 2 when choosing a strategy, with proportions oscillating around 0.5 (Fig. 2.c). In scenario

3, populations consistently evolved to choose a kleptoparasitic-scrounger strategy in the presence of handlers (Fig. 2c.). This proportion was reduced at very low growth rates ($r_{base} < 0.01$; Fig. 2.c).

The Evolution of Kleptoparasitism

main point: kleptoparasitism evolves through pre-adaptation to moving towards handlers

Generalised Functional Response

The effect of individual and prey-item density on per-capita intake changed non-linearly in relation to r_{base} (Figure 3). In scenario 1, the effect of individuals on producer per-capita intake (coefficient β_2) was initially negative at low growth rates, and then slightly positive (max. $\beta_2 \approx 0.5$) for intermediate, high and very high growth rates. The effect of items (coefficient β_1) declined from low positive values to zero with increasing r_{base}. In scenario 2, β_2 for both W_p and W_s was near zero for $r_{base} < 0.05$, increased rapidly for for $r_{base} \in 0.05, 0.075, 0.1$, and declined to < 0.5 for $r_{base} = 0.25$. The β_1 (items) was at or near zero across all r_{base} for both W_p and W_s. In the flexible-strategy case, β_2 showed a hump-shaped relationship with r_{base} for both W_p and W_s, with negative values at low growth rates, the highest values at intermediate growth rates, and low values at the highest growth rate. The effect of items (β_1) declined from low positive values to zero with increasing r_{base}.

Ecological Models Mask Behavioural Mechanisms

Evolved behavioural mechanisms are very poorly captured by phenomenological models of functional response coefficients for individuals and prey-items. Across regrowth rates, models of intake rate would predict that prey-item abundance has little to no effect with $\beta_1 \approx 0$, while competitor density (coefficient β_2) would be expected to have an equal or stronger effect. These models predict that individuals should not select for prey-items, and move away from each other

at low regrowth rates, while moving towards each other at higher regrowth rates. However, individuals are not neutral to prey-items, instead showing a strong preference at all regrowth rates. Further, individuals' response to other individuals is based on the sensed behavioural state; populations evolve to move towards handlers and away from non-handlers across a range of regrowth rates. At low regrowth rates, items are expected to be scarce across the landscape, and item densities are unreliable cues of cell quality. Yet individual immobility while handling prey leads to the positive correlation of individual densities and cell quality, as producers are converted to handlers more rapidly on cells with higher r. When direct cues are unreliable, individuals can use the foraging status of conspecifics as public information to detect a landscape quality gradient. Thus even though individual intake is negatively affected by the presence of other individuals generally, a strong preference for moving towards handlers evolves. This social-information use may explain why animal groups are apparently larger than predicted on low-productivity landscapes without invoking extrinsic effects such as predation risk. At high regrowth rates, the probability of finding a food item is invariant with the number of potential competitors, food items are good cues of cell quality, and selection for individuals becomes neutral. Nonetheless, handling-immobility ensures that most producer-handler conversions occur in the presence of already-handling individuals, giving rise to the spurious inference of a facilitative effect of individuals on intake.

Emergence of a Third Trophic Level

main points: Kleptoparasites evolve when allowed to do so — kleptoparasite intake depends only on the number of individuals — kleptoparasite intake is highest when cells have few kleptoparasites and many producers

Spatial Distribution of Individuals and Prey

Individual Distributions. There number of individuals on a cell increased with its growth rate r, but there was substantial variation across cells with the same r. This variation was larger with increasing r since there were fewer cells with higher r. In the producer-only case, individual abundance showed a linear relationship with cell quality, with the slope increasing with the simulation growth rate r_{base}. When two strategies were allowed however, there were strong differences in how they were distributed across cell qualities. In the fixed-strategy case, the abundance of producer individuals was uniformly low across cell qualities, while the abundance of scrounging kleptoparasites had a sigmoidal relationship with quality, mediated by r_{base}. In the flexible-strategy case, the use of either strategy was nearly invariant with cell quality. At very low r_{base} (0.001) the kleptoparasitic strategy was more ofen used than the producer strategy, while at higher r_{base}, the producer strategy was more common across cell quality.

Consequences for Prey Item Distribution. The distributon of items G varied considerably between scenarios and simulation-specific baseline growth rates r_{base}. In the **scenario 1** G was insensitive to r, and items were uniformly distributed across cells of different growth rates. G was not significantly different among simulations with different r_{base}. In the **scenario 2** G increased strongly with r, and the curve of G r varied with r_{base}. The G r transformed from roughly linear (r_{base} = 0.001), to exponential (r_{base} = 0.01), and finally to sigmoidal ($r_{base} \in$ 0.03, 0.05) [see Figure X]. In the **scenario 3** G varied only weakly across cells with different r, and the G r response had a positive slope only for the highest r_{base} of 0.03 and 0.05.

Deviations from the IFD

main points: undermatching due to difficulty in detecting gradients — evolved functional response does not match classical models

Discussion

Conclusion

Acknowledgments

The authors thank Hanno Hildenbrandt for contributing to the coding of the simulation model *Kleptomove*; Matteo Pederboni for contributing to the initial stages of the simulation model; and members of the Modelling Adaptive Response Mechanisms Group and of the Theoretical Biology department at the University of Groningen for helpful discussions on the manuscript.

Literature Cited

de Jager, M., J. van de Koppel, E. J. Weerman, and F. J. Weissing. 2020. Patterning in Mussel Beds Explained by the Interplay of Multi-Level Selection and Spatial Self-Organization. Frontiers in Ecology and Evolution 8.

de Jager, M., F. J. Weissing, P. M. J. Herman, B. A. Nolet, and J. van de Koppel. 2011. Lévy Walks Evolve Through Interaction Between Movement and Environmental Complexity. Science 332:1551–1553.

Ens, B. J., P. Esselink, and L. Zwarts. 1990. Kleptoparasitism as a problem of prey choice: A study on mudflat-feeding curlews, Numenius arquata. Animal Behaviour 39:219–230.

Levin, S. A. 1992. The Problem of Pattern and Scale in Ecology: The Robert H. MacArthur Award Lecture. Ecology 73:1943–1967.

Meer, J. V. D., and B. J. Ens. 1997. Models of Interference and Their Consequences for the Spatial Distribution of Ideal and Free Predators. The Journal of Animal Ecology 66:846.

Vahl, W. K., T. Lok, J. van der Meer, T. Piersma, and F. J. Weissing. 2005*a*. Spatial clumping of

342 food and social dominance affect interference competition among ruddy turnstones. Behavioral
343 Ecology 16:834–844.

344 Vahl, W. K., J. van der Meer, F. J. Weissing, D. van Dullemen, and T. Piersma. 2005*b*. The
345 mechanisms of interference competition: Two experiments on foraging waders. Behavioral
346 Ecology 16:845–855.

347 ———. 2005*c*. The mechanisms of interference competition: Two experiments on foraging
348 waders. Behavioral Ecology 16:845–855.

Appendix A: Supplementary Figures

Fox–dog encounters through the ages

Appendix B: Additional Methods

Measuring the height of fox jumps without a meterstick

Tables

Figure legends

Online figure legends

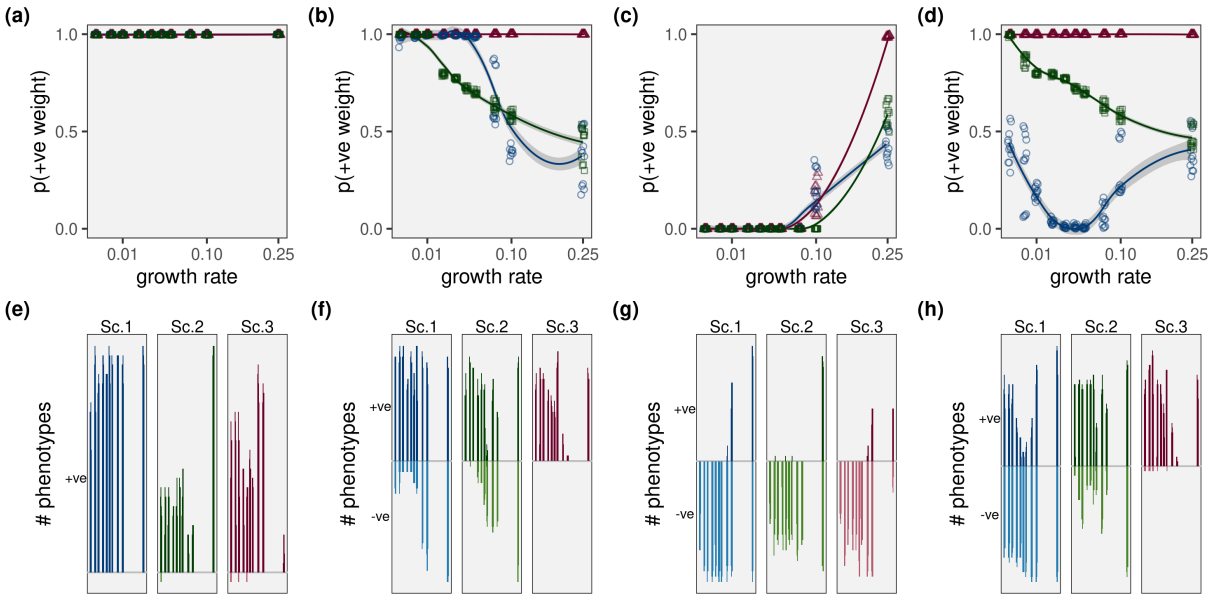

Figure 1: Proportion of evolved populations moving towards environmental cues in deciding movement, across different regrowth rates. Panels **(a – d)** show the proportion of individuals with positive weights for each cue: **(a)** non-handling individuals, **(b)** handling individuals, **(c)** prey items, and **(d)** individuals overall. Colours and shapes represent scenarios (blue circles: *producers-only*; green triangles: *fixed-strategy*; red squares: *flexible-strategy*). Each point represents a single generation between 990 and 998 in 3 replicates. Panels **(e – h)** show the number of distinct values for each weight in the population in panels **(a – d)** separated by the sign (positive or negative): **(e)** non-handling individuals, **(f)** handling individuals, **(g)** prey items, and **(h)** individuals overall. Bar colours represent scenarios (blue: *producers-only*; green: *fixed-strategy*; red: *flexible-strategy*), while the hue represents the sign (light: positive, dark: negative). Individuals across scenarios and growth rates evolve to always move towards food items (**a, e**). The preference for handlers decreases with growth rate in scenarios 1 and 2, but is consistently positive in scenario 3 (**b, f**). Non-handler avoidance decreases only at high growth rates (**c, g**). While the overall preference for individuals depends on the growth rate in scenarios 1 (inverse hump shape) and 2 (linear decline), individuals in scenario 3 always move towards each other (**d, h**).

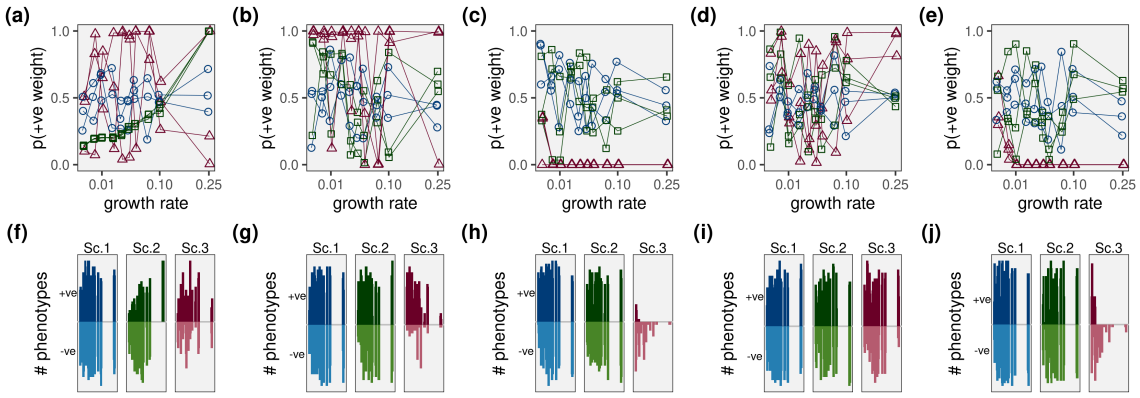

Figure 2: The proportion of individuals choosing a foraging strategy based on environmental cues is not linked to the regrowth rate. Panels **(a – e)** show the proportion of individuals with positive weights for each cue: **(a)** bias, **(b)** non-handling individuals, **(c)** handling individuals, **(d)** prey items, and **(e)** all cues combined. Colours and shapes represent scenarios (blue circles: *producers-only*; green triangles: *fixed-strategy*; red squares: *flexible-strategy*). Lines connect similarly numbered replicates across r_{base}, but these are entirely independent simulations. Panels **(f – j)** show the number of distinct values for each weight in the population in panels **(a – e)** separated by the sign (positive or negative): **(f)** bias, **(g)** non-handling individuals, **(h)** handling individuals, **(i)** prey items, and **(j)** all cues combined. Bar colours represent scenarios (blue: *producers-only*; green: *fixed-strategy*; red: *flexible-strategy*), while the hue represents the sign (light: positive, dark: negative). Individuals' weights in scenario 1 evolve neutrally since they are only allowed a producer strategy. However, scenario 2 also results in neutral evolution of all weights except f_b, with a larger proportion of individuals biased towards producing at high r_{base}. Almost all individuals in scenario 3 choose to steal except at very low r_{base}, with f_h the strongest contributor to the decision.

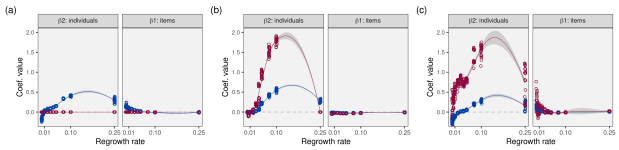

Figure 3: The effect of individuals and items on per-capita intake rate differs across regrowth rates and individual strategy. Across scenarios (**a**: producers-only, **b**: fixed-strategy, and **c**: flexible-strategy) and strategies (blue: producer, red: kleptoparasite), the effect of individuals (β_2) and prey items (β_1) is hump-shaped with respect to regrowth rates. It is initially negative or zero at low regrowth rates, and increases to positive values for intermediate and high regrowth rates, before declining at extremely high levels of prey regrowth.